

Dineutrino modes probing lepton flavor violation

Rigo Bause,^a Hector Gisbert,^{a,*} Marcel Golz^a and Gudrun Hiller^a

^a*Fakultät für Physik, TU Dortmund,*

Otto-Hahn-Str. 4, D-44221 Dortmund, Germany

E-mail: rigo.bause@tu-dortmund.de, hector.gisbert@tu-dortmund.de,

marcel.golz@tu-dortmund.de, ghiller@physik.uni-dortmund.de

$SU(2)_L$ -invariance links charged dilepton $\bar{q} q' \ell^+ \ell^-$ and dineutrino $\bar{q} q' \bar{\nu} \nu$ couplings. This connection can be established using the Standard Model Effective Field Theory framework, and allows to perform complementary experimental tests of lepton universality and charged lepton flavor conservation with flavor-summed dineutrino observables. We present its phenomenological implications for the branching ratios of rare charm decays $c \rightarrow u \nu \bar{\nu}$ and rare B decays $b \rightarrow s \bar{\nu} \nu$ decays.

*The European Physical Society Conference on High Energy Physics (EPS-HEP2021),
26-30 July 2021*

Online conference, jointly organized by Universität Hamburg and the research center DESY

*Speaker

1. Introduction

Flavor-changing neutral currents (FCNCs) of q^α and q^β quarks induced by $|\Delta q^\alpha| = |\Delta q^\beta| = 1$ processes represent excellent probes of New Physics (NP) beyond the Standard Model (SM). Their weak loop suppression triggered by the Glashow-Iliopoulos-Maiani (GIM) mechanism and Cabibbo-Kobayashi-Maskawa (CKM) hierarchies, not necessarily present in SM extensions, can result in large experimental deviations from the SM predictions alluding to a breakdown of SM symmetries. In addition, its environment is enriched with further tests if leptons are involved, that is $q_\alpha q_\beta \ell_i^+ \ell_j^-$ and $q_\alpha q_\beta \bar{\nu}_i \nu_j$. We exploit the $SU(2)_L$ -link between left-handed charged lepton and neutrino couplings, which may be used to assess charged lepton flavor conservation (cLFC) and lepton universality (LU) quantitatively using flavor-summed dineutrino observables [1]. This link (3) is presented for $|\Delta q^\alpha| = |\Delta q^\beta| = 1$ processes, but we stress that it holds analogously for other conserved quark transitions, both in the up- and down-sector.

These proceedings are organized as follows: In Section 2, we present the effective theory framework where the $SU(2)_L$ -link between neutrino and charged lepton couplings is derived. In Sections 3 and 4, we work out its phenomenological implications for charm and beauty, respectively. The conclusions are drawn in Section 5. The results are based on Refs. [1–3], we refer there for further details.

2. $SU(2)_L$ -link between dineutrino and charged dilepton couplings

At lowest order in the SM effective field theory (SMEFT), the Lagrangian accounting for semileptonic (axial-)vector four-fermion operators is given by [4],

$$\mathcal{L}_{\text{eff}} \supset \frac{C_{\ell q}^{(1)}}{v^2} \bar{Q} \gamma_\mu Q \bar{L} \gamma^\mu L + \frac{C_{\ell q}^{(3)}}{v^2} \bar{Q} \gamma_\mu \tau^a Q \bar{L} \gamma^\mu \tau^a L + \frac{C_{\ell u}}{v^2} \bar{U} \gamma_\mu U \bar{L} \gamma^\mu L + \frac{C_{\ell d}}{v^2} \bar{D} \gamma_\mu D \bar{L} \gamma^\mu L. \quad (1)$$

Reading off couplings to dineutrinos (C_A^N) and charged dileptons (K_A^N) by writing the operators (1) into $SU(2)_L$ -components, one obtains

$$\begin{aligned} C_L^U = K_L^D &= \frac{2\pi}{\alpha} \left(C_{\ell q}^{(1)} + C_{\ell q}^{(3)} \right), & C_R^U = K_R^U &= \frac{2\pi}{\alpha} C_{\ell u}, \\ C_L^D = K_L^U &= \frac{2\pi}{\alpha} \left(C_{\ell q}^{(1)} - C_{\ell q}^{(3)} \right), & C_R^D = K_R^D &= \frac{2\pi}{\alpha} C_{\ell d}, \end{aligned} \quad (2)$$

where $N = U$ ($N = D$) represents the up-quark sector (down-quark sector), and $A = L(R)$ denotes left- (right-) handed quark currents. Interestingly, $C_R^N = K_R^N$ holds model-independently, while C_L^N is not fixed by K_L^N in general due to the different relative signs of $C_{\ell q}^{(1)}$ and $C_{\ell q}^{(3)}$. Expressing Eqs. (2) in the mass basis, that is $C_L^N = W^\dagger \mathcal{K}_L^N W + \mathcal{O}(\lambda)$, $C_R^N = W^\dagger \mathcal{K}_R^N W$ where W is the Pontecorvo-Maki-Nakagawa-Sakata (PMNS) matrix and $\lambda \sim 0.2$ the Wolfenstein parameter, and summing lepton flavors i, j incoherently, one obtains the following identity [1]

$$\sum_{\nu=i,j} \left(|C_L^{Nij}|^2 + |C_R^{Nij}|^2 \right) = \sum_{\ell=i,j} \left(|\mathcal{K}_L^{Mij}|^2 + |\mathcal{K}_R^{Nij}|^2 \right) + \mathcal{O}(\lambda), \quad (3)$$

between charged lepton couplings $\mathcal{K}_{L,R}$ and neutrino ones $C_{L,R}$.¹ Here, we use $N, M = U, D$ when the link is exploited for neutrino couplings in the up-quark sector, while $N, M = D, U$ for

¹Wilson coefficients in calligraphic style denote those for mass eigenstates.

the down-quark sector. Eq. (3) allows the prediction of dineutrino rates for different leptonic flavor structures $\mathcal{K}_{L,R}^{Nij}$,

- i) $\mathcal{K}_{L,R}^{Nij} \propto \delta_{ij}$, *i.e.* lepton-universality (LU),
- ii) $\mathcal{K}_{L,R}^{Nij}$ diagonal, *i.e.* charged lepton flavor conservation (cLFC),
- iii) $\mathcal{K}_{L,R}^{Nij}$ arbitrary,

which can be probed with lepton-specific measurements. In the following sections, we use the following notation *i.e.* $\mathcal{K}_{L,R}^{bsij} = \mathcal{K}_{L,R}^{D_{23}ij}$, $C_{L,R}^{bsij} = C_{L,R}^{D_{23}ij}$, etc., to improve the readability.

	ee	$\mu\mu$	$\tau\tau$	$e\mu$	$e\tau$	$\mu\tau$
$R^{\ell\ell'}$	21	6.0	77	6.6	59	70
$\delta R^{\ell\ell'}$	19	5.4	69	5.7	55	63
$r^{\ell\ell'}$	39	11	145	12	115	133

Table 1: Bounds on $|\Delta c| = |\Delta u| = 1$ parameters $R^{\ell\ell'}$ and $\delta R^{\ell\ell'}$ from Eqs. (4), as well as their sum, $r^{\ell\ell'} = R^{\ell\ell'} + \delta R^{\ell\ell'}$. Table taken from Ref. [2].

3. Predictions for charm

In this section, we study the implications of (3) for $c \rightarrow u \nu \bar{\nu}$ dineutrino transitions, where the situation is exceptional as the SM amplitude is fully negligible due to an efficient GIM-suppression [5] and the current lack of experimental constraints. We use upper limits on $\mathcal{K}_A^{N\ell\ell'}$ from high- p_T [6, 7], which allow to set constraints on

$$R^{\ell\ell'} = |\mathcal{K}_L^{sd\ell\ell'}|^2 + |\mathcal{K}_R^{cu\ell\ell'}|^2, \quad R_{\pm}^{\ell\ell'} = |\mathcal{K}_L^{sd\ell\ell'} \pm \mathcal{K}_R^{cu\ell\ell'}|^2, \quad (4)$$

$$\delta R^{\ell\ell'} = 2\lambda \operatorname{Re} \left\{ \mathcal{K}_L^{sd\ell\ell'} \mathcal{K}_L^{ss\ell\ell'^*} - \mathcal{K}_L^{sd\ell\ell'} \mathcal{K}_L^{dd\ell\ell'^*} \right\},$$

which directly enter in $c \rightarrow u \nu \bar{\nu}$ branching ratios. Upper limits on $R^{\ell\ell'}$, $\delta R^{\ell\ell'}$ and their sum $r^{\ell\ell'} = R^{\ell\ell'} + \delta R^{\ell\ell'}$ are provided in Table 1. Since the neutrino flavors are not tagged, the branching ratio is obtained by an incoherent sum

$$\mathcal{B}(c \rightarrow u \nu \bar{\nu}) = \sum_{i,j} \mathcal{B}(c \rightarrow u \nu_i \bar{\nu}_j) \propto x_{uc}, \quad (5)$$

where $x_{uc} = \sum_{i,j} (|C_L^{Uij}|^2 + |C_R^{Uij}|^2)$. Using (3) with $N, M = U, D$ and Table 1, we obtain upper limits for the different benchmarks *i-iii*):

$$x_{uc} = 3 r^{\mu\mu} \lesssim 34, \quad (\text{LU}) \quad (6)$$

$$x_{uc} = r^{ee} + r^{\mu\mu} + r^{\tau\tau} \lesssim 196, \quad (\text{cLFC}) \quad (7)$$

$$x_{uc} = r^{ee} + r^{\mu\mu} + r^{\tau\tau} + 2(r^{e\mu} + r^{e\tau} + r^{\mu\tau}) \lesssim 716. \quad (8)$$

Since dimuon bounds are the most stringent ones, see Table 1, they set the LU-limit (6). Experimental measurements above the upper limit in (6) would indicate a breakdown of LU, while values above the limit in (7) would imply a violation of cLFC. Corresponding upper limits on branching ratios of dineutrino modes of a charmed hadron h_c into a final hadronic state F ,

$$\mathcal{B}(h_c \rightarrow F \nu \bar{\nu}) = A_+^{h_c F} x_{cu}^+ + A_-^{h_c F} x_{cu}^-, \quad (9)$$

are provided in Table 2 for several decays modes. The $A_{\pm}^{h_c F}$ coefficients in Eq. (9) are given in the second column of Table 2. Using the limits (6), (7), (8), together with Eq. (9) and the values of $A_{\pm}^{h_c F}$, we obtain upper limits on branching ratios for the three flavor scenarios $\mathcal{B}_{\text{LU}}^{\text{max}}$, $\mathcal{B}_{\text{cLFC}}^{\text{max}}$, and \mathcal{B}^{max} . A branching ratio measurement \mathcal{B}_{exp} within $\mathcal{B}_{\text{LU}}^{\text{max}} < \mathcal{B}_{\text{exp}} < \mathcal{B}_{\text{cLFC}}^{\text{max}}$ would be a clear signal of LU violation. In contrast, a branching ratio above $\mathcal{B}_{\text{cLFC}}^{\text{max}}$ would imply a breakdown of cLFC.

$h_c \rightarrow F$	$A_+^{h_c F}$ [10 ⁻⁸]	$A_-^{h_c F}$ [10 ⁻⁸]	$\mathcal{B}_{\text{LU}}^{\text{max}}$ [10 ⁻⁷]	$\mathcal{B}_{\text{cLFC}}^{\text{max}}$ [10 ⁻⁶]	\mathcal{B}^{max} [10 ⁻⁶]
$D^0 \rightarrow \pi^0$	0.9	–	6.1	3.5	13
$D^+ \rightarrow \pi^+$	3.6	–	25	14	52
$D_s^+ \rightarrow K^+$	0.7	–	4.6	2.6	9.6
$D^0 \rightarrow \pi^0 \pi^0$	$O(10^{-3})$	0.21	1.5	0.8	3.1
$D^0 \rightarrow \pi^+ \pi^-$	$O(10^{-3})$	0.41	2.8	1.6	5.9
$D^0 \rightarrow K^+ K^-$	$O(10^{-6})$	0.004	0.03	0.02	0.06
$\Lambda_c^+ \rightarrow p^+$	1.0	1.7	18	11	39
$\Xi_c^+ \rightarrow \Sigma^+$	1.8	3.5	36	21	76
$D^0 \rightarrow X$	2.2	2.2	15	8.7	32
$D^+ \rightarrow X$	5.6	5.6	38	22	80
$D_s^+ \rightarrow X$	2.7	2.7	18	10	38

Table 2: Coefficients $A_{\pm}^{h_c F}$, as defined in (9), and model-independent upper limits on $\mathcal{B}_{\text{LU}}^{\text{max}}$, $\mathcal{B}_{\text{cLFC}}^{\text{max}}$, \mathcal{B}^{max} from (6), (7) and (8), respectively, corresponding to the lepton flavor symmetry benchmarks *i-iii*). Table taken from Ref. [2].

4. Testing lepton universality with $b \rightarrow s \nu \bar{\nu}$

In this section we study $b \rightarrow s \nu \bar{\nu}$ transitions and their interplay with $b \rightarrow s \ell^+ \ell^-$ transitions routed by (3). The branching ratios for $B \rightarrow V \nu \bar{\nu}$ and $B \rightarrow P \nu \bar{\nu}$ decays in the LU limit are given by

$$\mathcal{B}(B \rightarrow V \nu \bar{\nu})_{\text{LU}} = A_+^{BV} x_{bs,\text{LU}}^+ + A_-^{BV} x_{bs,\text{LU}}^-, \quad \mathcal{B}(B \rightarrow P \nu \bar{\nu})_{\text{LU}} = A_+^{BP} x_{bs,\text{LU}}^+, \quad (10)$$

where $x_{bs,\text{LU}}^{\pm} = 3 |C_{\text{SM}}^{bs\ell\ell} + \mathcal{K}_L^{t\ell\ell} \pm \mathcal{K}_R^{bs\ell\ell}|^2$, and the values of A_{\pm}^{BV} and A_+^{BP} for different modes can be found in Ref. [3]. We obtain two solutions for the coupling $\mathcal{K}_L^{t\ell\ell}$ when we solve $\mathcal{B}(B \rightarrow P \nu \bar{\nu})_{\text{LU}}$ in Eq. (10). Plugging them into Eq. (10) results in a correlation between both LU branching ratios [3]

$$\mathcal{B}(B \rightarrow V \nu \bar{\nu})_{\text{LU}} = \frac{A_+^{BV}}{A_+^{BP}} \mathcal{B}(B \rightarrow P \nu \bar{\nu})_{\text{LU}} + 3 A_-^{BV} \left| \sqrt{\frac{\mathcal{B}(B \rightarrow P \nu \bar{\nu})_{\text{LU}}}{3 A_+^{BP}}} \mp 2 \mathcal{K}_R^{bs\ell\ell} \right|^2. \quad (11)$$

The most stringent limits on $\mathcal{K}_R^{bs\ell\ell}$ are given for $\ell\ell = \mu\mu$. Performing a 6D global fit of the semileptonic Wilson coefficients $C_{(7,9,10),\mu}^{(\prime)}$ to the current experimental data on $b \rightarrow s \mu^+ \mu^-$ data (excluding $R_{K^{(*)}}$ which can be polluted by NP effects in electron couplings), we obtain the following 1σ fit value [3]

$$\mathcal{K}_R^{bs\ell\ell} = V_{tb}V_{ts}^* (0.46 \pm 0.26). \quad (12)$$

Fig. 1 displays the correlation between $\mathcal{B}(B^0 \rightarrow K^{*0}\nu\bar{\nu})$ and $\mathcal{B}(B^0 \rightarrow K^0\nu\bar{\nu})$, cf. Eq. (11). The SM predictions $\mathcal{B}(B^0 \rightarrow K^{*0}\nu\bar{\nu})_{\text{SM}} = (8.2 \pm 1.0) \cdot 10^{-6}$, $\mathcal{B}(B^0 \rightarrow K^0\nu\bar{\nu})_{\text{SM}} = (3.9 \pm 0.5) \cdot 10^{-6}$ [3] are depicted as a blue diamond with their 1σ uncertainties (blue bars). We have scanned $\mathcal{K}_R^{bs\mu\mu}$, $A_{\pm}^{B^0K^{*0}}$, and $A_{+}^{B^0K^0}$ within their 1σ (2σ) regions in Eq. (10), resulting in the dark red region (dashed red lines) which represents the LU region, numerically [3]

$$\frac{\mathcal{B}(B^0 \rightarrow K^{*0}\nu\bar{\nu})}{\mathcal{B}(B^0 \rightarrow K^0\nu\bar{\nu})} = 1.7 \dots 2.6 \quad (1.3 \dots 2.9). \quad (13)$$

Interestingly, a branching ratio measurement outside the red region would clearly signal evidence for LU violation, but if a future measurement is instead inside this region, this may not necessarily imply LU conservation. Outside the light green region the validity of our effective field theory (EFT) framework gets broken [3]. More stringent limits for specific LU SM extensions are depicted as benchmarks, resulting in best fit values (markers) and 1σ regions (ellipses) for Z' (red star), LQ representations S_3 (pink pentagon) and V_3 (celeste triangle) from $b \rightarrow s \mu^+ \mu^-$ global fits, see Ref. [3] for details. The current experimental 90% CL upper limits, $\mathcal{B}(B^0 \rightarrow K^{*0}\nu\bar{\nu})_{\text{exp}} < 1.8 \cdot 10^{-5}$ [8] and $\mathcal{B}(B^0 \rightarrow K^0\nu\bar{\nu})_{\text{exp}} < 2.6 \cdot 10^{-5}$ [8], are displayed by hatched bands. The gray bands represent the derived EFT limits, $\mathcal{B}(B^0 \rightarrow K^0\nu\bar{\nu})_{\text{derived}} < 1.5 \cdot 10^{-5}$, from Ref. [3]. A measurement between gray and hatched area would infer a clear hint of NP not covered by our EFT framework, *i.e.* *light particles*. The projected experimental sensitivity (10% at the chosen point) of Belle II with 50 ab^{-1} is illustrated by the yellow boxes [9]. Similar conclusions can be drawn in $b \rightarrow d \nu\bar{\nu}$ decay [3].

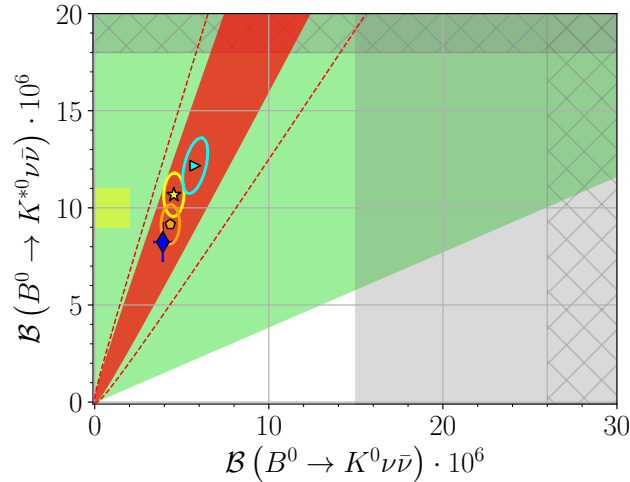


Figure 1: Correlation between $\mathcal{B}(B^0 \rightarrow K^{*0}\nu\bar{\nu})$ and $\mathcal{B}(B^0 \rightarrow K^0\nu\bar{\nu})$. Details are given in the main text. Figure taken from Ref. [3].

5. Conclusions

$SU(2)_L$ -invariance relates dineutrinos $\bar{q} q' \bar{\nu} \nu$ and charged dilepton couplings $\bar{q} q' \ell^+ \ell^-$ in a model-independent way. This link (3) allows probing lepton flavor structure in dineutrino observables in three benchmarks: lepton universality, charged lepton flavor conservation and lepton flavor violation. The link has been exploited for the rare charm and B decays, resulting in novel tests of the aforementioned symmetries, see Table 2 and Eq. (13), respectively. Our predictions are well-suited for the experiments Belle II [9], BES III [10], and future e^+e^- -colliders, such as an FCC-ee running at the Z [11], and could offer some insight on the persistent anomalies in B decays.

Acknowledgments

We want to thank the organizers for their effort to make this conference such a successful event. This work is supported by the *Studienstiftung des Deutschen Volkes* (MG) and the *Bundesministerium für Bildung und Forschung – BMBF* (HG).

References

- [1] R. Bause, H. Gisbert, M. Golz and G. Hiller, [arXiv:2007.05001 [hep-ph]].
- [2] R. Bause, H. Gisbert, M. Golz and G. Hiller, Phys. Rev. D **103** (2021) no.1, 015033 [arXiv:2010.02225 [hep-ph]].
- [3] R. Bause, H. Gisbert, M. Golz and G. Hiller, [arXiv:2109.01675 [hep-ph]].
- [4] B. Grzadkowski, M. Iskrzynski, M. Misiak and J. Rosiek, JHEP **10** (2010), 085 [arXiv:1008.4884 [hep-ph]].
- [5] G. Burdman, E. Golowich, J. L. Hewett and S. Pakvasa, Phys. Rev. D **66**, 014009 (2002) [hep-ph/0112235].
- [6] J. Fuentes-Martin, A. Greljo, J. Martin Camalich and J. D. Ruiz-Alvarez, JHEP **11** (2020), 080. [arXiv:2003.12421 [hep-ph]].
- [7] A. Angelescu, D. A. Faroughy and O. Sumensari, Eur. Phys. J. C **80**, no.7, 641 (2020) [arXiv:2002.05684 [hep-ph]].
- [8] P.A. Zyla *et al.* [Particle Data Group], PTEP **2020**, no.8, 083C01 (2020)
- [9] E. Kou *et al.* [Belle-II Collaboration], PTEP **2019**, no. 12, 123C01 (2019) [arXiv:1808.10567 [hep-ex]].
- [10] M. Ablikim *et al.*, Chin. Phys. C **44** (2020) no.4, 040001 [arXiv:1912.05983 [hep-ex]].
- [11] A. Abada *et al.* [FCC Collaboration], Eur. Phys. J. C **79**, no. 6, 474 (2019).